Functional Consequences of the Oligomeric Form of the Membrane-Bound Gastric H,K-ATPase†

Jai Moo Shin,*,‡ Gerhard Grundler,§ Jörg Senn-Bilfinger,§ Wolfgang Alexander Simon,§ and George Sachs‡

Department of Physiology and Medicine, University of California at Los Angeles, and VA Greater Los Angeles Healthcare System, Los Angeles, California 90073, and ALTANA Pharma AG, Konstanz, Germany

Received July 12, 2005; Revised Manuscript Received October 20, 2005

ABSTRACT: Cross-linking and two-dimensional crystallization studies have suggested that the membrane-bound gastric H,K-ATPase might be a dimeric α,β-heterodimer. Effects of an oligomeric structure on the characteristics of E_1, E_2, and phosphoenzyme conformations were examined by measuring binding stoichiometries of acid-stable phosphorylation (EP) from [γ-^{32}P]ATP or $^{32}P_i$ or of binding of [γ-^{32}P]ATP and of a K^+-competitive imidazonaphthyridine (INT) inhibitor to an enzyme preparation containing ~ 5 nmol of ATPase/mg of protein. At <10 μM MgATP, E_1[ATP]·Mg·(H^+):E_2 is formed at a high-affinity site, and is then converted to E_1P·Mg·(H^+):E_2 and then to E_2P·Mg:E_1 with luminal proton extrusion. Maximal acid-stable phosphorylation yielded 2.65 nmol/mg of protein. Luminal K^+-dependent dephosphorylation returns this conformation to the E_1 form. At high MgATP concentrations (>0.1 mM), the oligomer forms E_2P·Mg:E_1[ATP]·Mg·(H^+). The sum of the levels of maximal EP formation and ATP binding was 5.3 nmol/mg. The maximal amount of [^{3}H]INT bound was 2.6 nmol/mg in the presence of MgATP, Mg^{2+}, Mg-P_i, or Mg-vanadate with complete inhibition of activity. K^+ displaced INT only in nigericin-treated vesicles, and thus, INT binds to the luminal surface of the E_2 form. INT-bound enzyme also formed 2.6 nmol of EP/mg at high ATP concentrations by formation of E_2·Mg·$(INT)_{exo}$:E_1[ATP]·Mg·(H^+) which is converted to E_2·Mg·$(INT)_{exo}$:E_1P·Mg·$(H^+)_{cyto}$, but this E_1P form was K^+-insensitive. Binding of the inhibitor fixes half the oligomer in the E_2 form with full inhibition of activity, while the other half of the oligomer is able to form E_1P only when the inhibitor is bound. It appears that the catalytic subunits of the oligomer during turnover in intact gastric vesicles are restricted to a reciprocal E_1:E_2 configuration.

P_2-type ATPases transport small cations across membranes via conformational changes in the catalytic protein driven by a cycle of phosphorylation and dephosphorylation of the enzymes. There has been much speculation about the possible significance of an oligomeric structure of some of the ATPases, especially the heterodimeric Na,K-ATPase and H,K-ATPase (*1*−*6*). Since the high-resolution crystal structure of the SR Ca-ATPase reveals only a single ATP binding site (*7*, *8*), kinetic anomalies such as half-of-site phosphorylation might be ascribed to inactive enzyme, half-site reactivity, or conformational restrictions resulting from association of the monomers in the oligomer. To delineate the possible effects of their quaternary structure on binding stoichiometries of one of the pumps, the gastric H,K-ATPase was measured with various ligands in different conformations of the enzyme.

The gastric H,K-ATPase, one of the two heterodimeric members of this ATPase family, catalyzes electroneutral H^+ for K^+ exchange to generate acid secretion by the stomach. It is composed of an α catalytic subunit, which contains the ion transport domain, and a six- or seven-site N-glycosylated β subunit which is necessary for maturation of the enzyme and plasma membrane delivery of the α subunit (*9*, *10*). In the presence of Mg^{2+}, phosphorylation proceeds via transfer of the γ-phosphate group of ATP to an aspartic acid residue of the enzyme (Asn^{385}), forming the acid-stable phosphoenzyme intermediate (EP)[1] (*11*−*13*). There are two main conformations of the phosphoenzyme: E_1P and E_2P. The E_1P form is sensitive to ADP but insensitive to K^+ and has the ion-binding sites facing inward. The E_2P form is sensitive to K^+ but insensitive to ADP, and its ion-binding sites face outward (*14*, *15*). The transfer of the γ-phosphate group of ATP to the enzyme results in the formation of E_1P along with binding of H^+ to the inward-facing ion-binding sites

† This work was supported in part by the U.S. Veterans Administration and NIH Grants DK46917, DK53462, DK58333, and DK17294 and in part by ALTANA Pharma AG.

* To whom correspondence should addressed: Membrane Biology Laboratory, VA Greater Los Angeles Healthcare System, 11301 Wilshire Blvd., Bldg. 113, Rm 324, Los Angeles, CA 90073. Telephone: (310) 268-4672. Fax: (310) 312-9478. E-mail: jaishin@ucla.edu.

‡ University of California at Los Angeles and VA Greater Los Angeles Healthcare System.

§ ALTANA Pharma AG.

[1] Abbreviations: CDTA, *trans*-1,2-diaminocyclohexane-*N*,*N*,*N*′,*N*′-tetraacetic acid; SCH28080, 3-(cyanomethyl)-2-methyl-8-(phenylmethoxy)imidazo[1,2-α]pyridine; INT, 6-(2-methoxyethoxy)-2,3-dimethyl-8-phenyl-6,7,8,9-tetrahydro-1,3α,9-triazacyclopenta[*a*]naphthalen-7-ol; TCA, trichloroacetic acid; PEG, polyethylene glycol; AcP_i, acetyl phosphate; P_i, inorganic phosphate; EP, phosphoenzyme intermediate; CDTA, *trans*-1,2-diaminocyclohexane-*N*,*N*,*N*′,*N*′-tetraacetic acid; EGTA, [ethylenebis(oxyethylenenitrilo)]tetraacetic acid; $C_{12}E_8$, octaethylene glycol dodecyl ether; TMA-Cl, tetramethylammonium chloride.

10.1021/bi051342q CCC: $30.25
Published on Web 11/17/2005

located in the membrane domain. E_1P then spontaneously converts to the E_2P form with luminal expulsion of H^+. The subsequent binding of K^+ to the outward-facing ion sites from the luminal side of the enzyme then results in dephosphorylation of the α subunit with, first, formation of an occluded form of K^+, where the cation is trapped in the membrane domain. This form then converts to E_1K^+, and K^+ is released to the cytoplasm upon rebinding of MgATP (*16*).

Although there is ~5 nmol of enzyme/mg of protein present in purified hog gastric vesicles, the reported maximal level of acid-stable phosphorylation has never exceeded ~2 nmol/mg of protein. This relatively low level of phosphorylation has traditionally been interpreted as indicating that either only 50% of enzyme in the preparation is active (*14*) or only half of the sites of the heterodimer can be phosphorylated to form an acid-stable phosphoenzyme. This latter hypothesis implies that there are structural associations between the two heterodimers of the oligomer, preventing identical conformations of each of the heterodimers from being present simultaneously. In support of the latter postulate, results of structural analysis of the membrane-bound enzyme using two-dimensional crystal analysis (*17*) and Cu^{2+}-phenanthroline cross-linking (*18*) and nondenaturing gel electrophoresis (*18*) suggested that the enzyme is present in the membrane as a dimeric heterodimer, $(\alpha\beta)_2$.

The enzyme can form 1 mol of acid-stable phosphoenzyme and 1 mol of acid-labile enzyme-bound ATP from 2 mol of enzyme (*19*). The H,K-ATPase has also been reported to have two ATP binding sites with different affinities (*19*−*22*). The K^+-competitive inhibitor SCH28080 binds to an extracytoplasmic domain (*23*−*25*). It inhibits K^+-stimulated ATPase activity by competing with K^+ for binding to the E_2P or E_2 conformation. SCH28080 has a higher affinity for the E_2P form (*25*), but the enzyme spontaneously converts to the E_2[SCH28080] form with release of P_i. At low ATP concentrations, ATP phosphorylation of E_2[SCH28080] is inhibited (*23*). However, at high ATP concentrations or in the presence of Mg and P_i, the SCH28080-bound enzyme can be phosphorylated to form acid-stable EP (*26*). Several reversible K^+-competitive inhibitors similar to SCH28080 have been synthesized. In this study, we used a ^{3}H-labeled imidazonaphthyridine homologue of SCH28080, namely INT, to investigate its effects and its binding stoichiometry. The imidazonaphthyridine has a fixed ring conformation to stabilize the known binding conformation of SCH28080 (*27*, *28*). This class of K^+-competitive inhibitor has been called the acid pump antagonist type, APA, to distinguish it from the covalent proton pump inhibitors (PPIs) that are in clinical use.

The binding data, along with the structural evidence that the enzyme is present as an oligomer, can be explained if there are two ATP binding sites in one functional dimeric oligomer of the gastric H,K-ATPase with different affinities.

The crystal structure of the homologous P-type ATPase, the SR Ca-ATPase, shows that there is only one ATP binding site on one catalytic subunit (*7*, *8*). The two distinct ATP binding sites must therefore reside on separate catalytic subunits of the H,K-ATPase. These data therefore suggest that the functional form of the enzyme in the apical membrane of the parietal cell may be an oligomer composed of a dimeric heterodimer with the association of the two

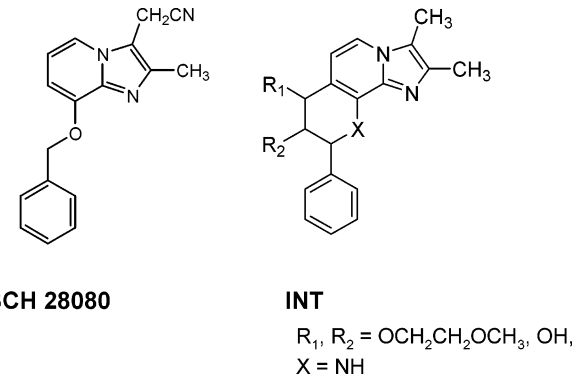

FIGURE 1: Structure of SCH28080 and the homologous fused labeled ring structure, INT, used in these studies. The INT compound fixes the benzene ring in the orthogonal position shown to be the active conformation of SCH28080.

catalytic subunits forcing an out-of-phase conformation, one in the E_1 conformation and the other in the E_2 conformation during enzyme turnover. This hypothesis can be tested by measuring the stoichiometry of binding of different ligands to the enzyme, either separately or in combination, under different conditions.

The heterodimer has an approximate molecular mass of 180 kDa. At 85% purity (*9*, *29*), since 1 mg of protein of hog gastric vesicles contains ~5 nmol of enzyme, this should provide ~5 nmol of reactive sites/mg of protein. To gain more insight into the functional properties of the H,K-ATPase in its native state in gastric membrane vesicles, we examined the maximal stoichiometry of binding of radioactive ATP to the enzyme and the ATP- or P_i-dependent acid-stable phosphorylation of the enzyme. Furthermore, we determined the maximal level of binding of a K^+-competitive inhibitor, INT, an imidazonaphthyridine homologue of SCH28080 (Figure 1), and the quantity of the acid-stable phosphoenzyme formed from high ATP concentrations in the presence of an inhibitor and the K^+ sensitivity of this acid-stable phosphoenzyme.

The studies reported here show that at high ATP concentrations, 5.3 nmol of total radioactivity was bound per milligram of the enzyme, indicating that, indeed, 1 mg of the enzyme contains ~5 nmol of ATP binding sites, close to the theoretical maximum of one site per heterodimer. In the presence of Mg^{2+}, however, only 2.7 nmol of acid-stable EP was formed. Hence, half of the enzyme formed acid-stable EP, while the other half of the enzyme bound an equal amount of labeled ATP without forming EP, as previously reported (*19*). The maximum level of Mg^{2+}-dependemt binding of the inhibitor, INT, was 2.6 nmol/mg of the enzyme with complete inhibition, although only half of the total enzyme sites were occupied. However, in the presence of a high concentration of MgATP and inhibitor, the stoichiometry of INT binding was equal to the stoichiometry of the acid-stable but K^+-insensitive phosphoenzyme, which formed to give also a net binding stoichiometry of ~5 nmol of binding sites/mg of enzyme.

The data described below are consistent with a structure in which the membrane-bound enzyme is an oligomer of two closely associated $(\alpha\beta)_2$ heterodimers with each of the heterodimers having different kinetic and binding characteristics due to this association. The oligomer of two

interacting ($\alpha\beta$) heterodimers appears to favor an $E_1 \cdot E_2$ conformation of the two heterodimers of the oligomer. This may be due to interference with the conformations of the nucleotide or actuator domain conformations in the two conformations (*7*, *8*, *18*).

MATERIALS AND METHODS

Hog Gastric H,K-ATPase Enzyme Preparation. The gastric H,K-ATPase was derived from hog gastric mucosa by a previously published method, which involves differential and density gradient centrifugation (*30*). All operations were carried out at 1−4 °C. The crude gastric mucosal membranes were collected from the stomach and homogenized in a solution of 0.25 M sucrose, 5 mM PIPES/Tris (pH 6.8), 1 mM EDTA, and 1 mM EGTA. The homogenate was centrifuged at 11 000 rpm in a Sorvall GSA rotor for 45 min. The pellet was discarded, and the supernatant was centrifuged at 34 000 rpm in a Beckman type 35 rotor for 1 h. The microsomal membrane pellet was resuspended in a solution of 0.25 M sucrose, 5 mM PIPES/Tris (pH 6.8), 1 mM EDTA, and 1 mM EGTA, and was purified on a step gradient sucrose solution, composed of 34% (w/v) sucrose, 5 mM PIPES/Tris (pH 6.8), 1 mM EDTA, and 1 mM EGTA, overlaid with a solution composed of 7.5% Ficoll, 0.25 M sucrose, 5 mM PIPES/Tris (pH 6.8), 1 mM EDTA, and 1 mM EGTA, using a SW 28 rotor at 27 000 rpm for 2 h. The vesicle fraction above the 7.5% Ficoll gradient was collected and diluted by adding 3 excess volumes of a solution of 5 mM PIPES/Tris (pH 6.8), 1 mM EDTA, and 1 mM EGTA. The suspension was centrifuged at 100000*g* for 1 h, and the pellet was resuspended in a solution of 0.25 M sucrose and 5 mM PIPES/Tris (pH 6.8).

The vesicles obtained have been shown to be more than 90% cytoplasmic side out. The Mg^{2+}-dependent activity was ~5.7 μmol mg^{-1} h^{-1}. The ion impermeability of the vesicles was determined by the difference in K^+ stimulation of ATPase activity in the presence of KCl alone and in the presence of KCl and the ionophore, nigericin. The activity in the presence of nigericin was 105 μmol of ATP hydrolyzed (mg of protein)$^{-1}$ h^{-1}, and in the absence of nigericin only 7.6 μmol mg^{-1} h^{-1}. Thus, more than 90% of the K^+-stimulated ATPase activity was dependent on the addition of the K^+ ionophore, nigericin, showing that this fraction of the vesicles was K^+-impermeant. The amount of P_i released was measured by the method of Yoda and Hokin (*31*), and the protein concentration was determined by a modified Lowry method (*32*) containing 0.1% SDS.

Measurement of Acid-Stable Phosphoenzyme Levels. Gastric vesicles (100−200 μg/mL) were incubated for 10 s at 20 °C in a buffer composed of 20 mM Tris/HCl (pH 7.0), 2 mM $MgCl_2$, and [γ-^{32}P]ATP (from 10 μM to 0.1 mM). An aliquot (0.4 mL) was taken and added to an ice-cold stop solution (1 mL) composed of 40% trichloroacetic acid, 10 mM phosphoric acid, and 1 mM ATP. This was immediately filtered through a nitrocellulose membrane filter (HAWP Millipore filter, 0.45 μm) prewetted with an ice-cold solution composed of 10% trichloroacetic acid and 20 mM phosphoric acid placed on top of a glass fiber filter. After being washed four times with 2.5 mL of an ice-cold solution composed of 10% trichloroacetic acid and 20 mM phosphoric acid, the membrane was placed in a 20 mL scintillation vial; dimethylacetamide (0.5 mL) was added to dissolve the membrane, and 10 mL of scintillation solvent was added and counted. Nonspecific P_i binding was assessed using a gastric vesicle suspension in a buffer composed of 20 mM Tris/HCl (pH 7.0), [γ-^{32}P]ATP (from 10 μM to 0.1 mM), and 5 mM CDTA with no Mg^{2+}, since Mg^{2+} is essential for phosphoenzyme formation. The acid-stable phosphoenzyme level was determined by subtracting the level of nonspecific binding obtained in the presence of CDTA-ATP from the total level of binding obtained in the presence of MgATP.

Measurement of the Total Amount of ^{32}P Bound to the Enzyme, Including Acid-Labile ^{32}P. The total amount of ^{32}P (acid-stable EP and [^{32}P]ATP) bound to the enzyme was measured using a centrifugation method, since washing excess trapped solution from the filters was unreliable (*19*). The gastric vesicles (0.1 mg/mL) were resuspended in a buffer composed of 20 mM Tris/HCl (pH 7.0), with or without 2 mM $MgCl_2$, with or without 10 mM CDTA, with 0.4 mM [γ-^{32}P]ATP/Tris (pH 7.0), with or without 5 μg of nigericin/mL, and with 50 mM [^{3}H]glucose. [^{3}H]Glucose was added to allow measurement of the trapped volume using a centrifugation method. The enzyme suspension was incubated at 20 °C for 1 min. The suspension was then centrifuged at 100000*g* for 10 min at 2 °C. The supernatant was immediately collected, and an aliquot of the supernatant was counted for ^{3}H and ^{32}P to obtain the ratio of free ^{32}P to ^{3}H in the solution. The membrane pellet was dissolved in 0.6 mL of 20 mM Tris/HCl and 0.5% SDS. The radioactivity of ^{3}H and ^{32}P of this membrane protein fraction was measured. On the basis of the ratio of ^{32}P to ^{3}H of the supernatant solution, the amount of solvent-trapped unbound ^{32}P was calculated from the counts of [^{3}H]glucose in the membrane protein fraction representing the liquid in the pellet and the amount of bound ^{32}P was obtained by subtracting the amount of unbound ^{32}P from the total amount of ^{32}P of the membrane protein. Since ^{32}P also results in counts in the tritium window in the scintillation counter, sufficient radioactive ^{3}H was added to minimize the effect of this ^{32}P crossover into the tritium window of the scintillation counter.

The amount of phosphoenzyme generated by inorganic phosphate was measured using the method described above. Here, the gastric vesicles (0.1 mg/mL) were incubated in a buffer composed of 20 mM Tris/HCl (pH 7.0), with or without 2 mM $MgCl_2$, with or without 10 mM CDTA, with 4 mM [^{32}P]phosphoric acid/Tris (pH 7.0), with or without 30 μg of nigericin/mL, and with 50 mM [^{3}H]glucose at 37 °C for 5 min or at 20 °C for 10 min.

Inhibition of ATPase Activity. ATPase activity was measured over a range of 0−10 mM KCl in the presence of different concentrations of INT (0−1 μM) and nigericin. The gastric vesicles (2−3 μg/mL) were resuspended in a buffer composed of 20 mM Tris/HCl (pH 7.0), 2 mM $MgCl_2$, KCl (0−10 mM), nigericin (1 μg/mL), and INT (0−1 μM). Background phosphate release was assessed using an enzyme suspension as described above but without $MgCl_2$. Activity was initiated by adding a final concentration of 2 mM ATP at 37 °C and incubation for 30 min. The amount of released inorganic phosphate was measured, and the ATPase activity was calculated.

The results obtained for the K^+-stimulated ATPase activity were fitted to equations describing patterns of competitive, noncompetitive, and mixed inhibition by least-squares fitting

using GraphPad Prism 4 (GraphPad Software Inc., San Diego, CA).

The IC_{50} was measured in the presence of 10 mM KCl and 2 mM KCl over a range of INT concentrations (0−1 μM).

Binding of INT to the Gastric H,K-ATPase. [^{3}H]INT binding studies were carried out at 20 or 1 °C. All experiments were performed in triplicate or more, and the average of the results was used for analysis.

In saturation experiments to determine the K_d value, the gastric vesicles (0.01−0.02 mg/mL) were resuspended in a buffer composed of 20 mM Tris/HCl (pH 7.0), 2 mM $MgCl_2$, and 2 mM ATP (pH 7.0, adjusted with Tris), and in the presence of increasing concentrations of [^{3}H]INT (from 0.1 nM to 1 μM). The level of nonspecific binding was determined in the presence of a 100-fold excess of unlabeled INT over the concentration range of [^{3}H]INT used. The enzyme suspension (1 mL) was incubated at 20 °C for 30 min and rapidly filtered through a nitrocellulose membrane filter (HAWP Millipore filter, 0.45 μm) prewet with a solution composed of 20 mM Tris/HCl (pH 7.0) and 10% PEG 3350 that was placed on top of a glass fiber filter. The membrane was washed five times with 2.5 mL of a buffer composed of 20 mM Tris/HCl (pH 7.0) and 10% PEG 3350 to remove unbound inhibitor. The membrane was placed in a 20 mL scintillation vial; dimethylacetamide (0.5 mL) was added to dissolve the membrane, and 14 mL of scintillation solvent was added and counted. Binding of [^{3}H]INT was assessed by subtracting the level of nonspecific binding of [^{3}H]INT, obtained in the presence of the 100-fold excess of nonradioactive INT, from the amounts of [^{3}H]INT bound to the membrane in the absence of the cold inhibitor. Binding of INT to K^+ leaky vesicles was assessed as described above in the presence of nigericin (5 μg/mL).

In KCl competition experiments, a fixed concentration of [^{3}H]INT (18 or 230 nM) was incubated in the presence of varying concentrations of KCl (0.001−300 mM) at 20 °C for 30 min in the presence and absence of nigericin (5 μg/mL). An aliquot at given concentration of KCl was taken out, and the radioactivity bound to the enzyme was measured as described above.

To investigate effects of various ligands on inhibitor binding, the gastric vesicles (0.01−0.1 mg/mL) were incubated at 20 °C for 30 min in a buffer composed of 20 mM Tris/HCl (pH 7.0) and different ligands such as 2 mM $MgCl_2$, 5 (or 10) mM CDTA, 2 mM ATP (pH 7.0, adjusted with Tris), 0.2 mM vanadate (pH 7.0), or 5 mM inorganic phosphate/Tris (pH 7.0) in the presence of increasing concentrations of [^{3}H]INT (from 100 nM to 2 μM).

To determine the effect of adding a Mg^{2+} chelating agent on reversal of INT that had already bound in the presence of Mg^{2+}, the gastric vesicles were incubated in a buffer composed of 2 mM ATP and 0.2 mM $MgCl_2$ in the presence of 100 nM [^{3}H]INT at 20 °C for 30 min. CDTA was then added to this suspension, to give a final concentration of 10 mM. An aliquot was then removed at timed intervals, and the quantity of INT bound was measured.

Effect of INT on the Phosphoenzyme. To determine the effect of the inhibitor on the formation of the acid-stable phosphoenzyme intermediate and total amount of ^{32}P bound to the enzyme, these were measured in the presence of INT. Intact gastric vesicles were incubated at 20 °C for 1 h in a buffer composed of 20 mM Tris/HCl (pH 7), with or without 2 mM $MgCl_2$, with or without 10 mM CDTA, with 10 μg of nigericin/mL, and with 2 μM [^{3}H]INT at a protein concentration of 100 μg/mL. Nonselective binding of INT was assessed by pretreatment with 0.2 mM unlabeled INT as described above. Using this INT-bound enzyme, [γ-^{32}P]-ATP was then added at a final concentration of 0.1 mM and the mixture incubated at 20 °C for 10, 20, 60, and 120 s. The amount of acid-stable EP was measured by the TCA precipitation and filtration method as described above.

To determine the total amount of ^{32}P bound to the enzyme, namely, both acid-stable EP and acid-labile ATP bound to the INT-bound enzyme, non-isotope-labeled INT was used for preparing the INT-bound enzyme. This enzyme preparation was then incubated in a buffer composed of 20 mM Tris/HCl (pH 7.0), with or without 2 mM $MgCl_2$, with or without 10 mM CDTA, with 0.4 mM [γ-^{32}P]ATP/Tris (pH 7.0), and with 50 mM [^{3}H]glucose again to determine the amount of trapped solvent after centrifugation and the total amount of ^{32}P bound to the enzyme measured as described above. The quantity of acid-stable EP formed under these conditions was measured by filtration of the TCA-precipitated protein as previously described.

Assessment of K^+-Stimulated Dephosphorylation. The addition of 1−10 mM K^+ to the phosphoenzyme formed at low ATP concentrations results in rapid dephosphorylation of the enzyme. In these experiments, the gastric vesicles were resuspended in a buffer composed of 20 mM Tris/HCl (pH 7.0), with or without 2 mM $MgCl_2$, with 5 μg of nigericin/mL, and with or without 5 mM CDTA at a protein concentration of 100 μg/mL at 20 °C. The enzyme suspension was incubated with 10 μM [γ-^{32}P]ATP for 10 s. The phosphoenzyme formed from 10 μM [γ-^{32}P]ATP after incubation for 10 s at 20 °C represents 100% EP in this particular experimental design. After addition of INT (2 or 10 μM), the enzyme suspension was incubated for 10 s at 20 °C and KCl (5 or 10 mM) was then added. An aliquot was taken at timed intervals, and the amount of phosphoenzyme was measured. The formation of phosphoenzyme is represented as % EP. Control represents EP formation in the absence of KCl and the inhibitor.

K^+-stimulated dephosphorylation of INT-bound enzyme was assessed using both low, 10 μM [γ-^{32}P]ATP, and high concentrations of ATP, 100 μM [γ-^{32}P]ATP. INT-bound enzyme was prepared by a 30 min incubation at 20 °C with 2 μM [^{3}H]INT at a protein concentration of 100 μg/mL as described above. [γ-^{32}P]ATP (10 or 100 μM) was added to the INT-bound enzyme suspension and the mixture incubated at 20 °C for 10 s (for 10 μM ATP) or 60 s (for 100 μM ATP). Then KCl (1−10 mM) was added. At timed intervals, an aliquot was taken out and the amount of acid-stable EP measured. Control experiments were carried out using the same method as described above except that TMA-Cl was used instead of KCl.

Materials. [^{3}H]INT (specific activity, 30 Ci/mmol) was a generous gift from G. Grundler (ALTANA Pharma AG). [γ-^{32}P]ATP (specific activity, 6000 Ci/mmol), [γ-^{32}P]phosphoric acid (specific activity, 200 mCi/mmol), and [^{3}H]-glucose (specific activity, 176 mCi/mg) were purchased from Amersham Biosciences. [γ-^{32}P]ATP (0.25 mCi) was diluted to 2 mL in 2 mM ATP/Tris (pH 7.0) to give a radioactivity of 0.125 mCi/mL and used within 5 days. [γ-^{32}P]Phosphoric

Table 1: Stoichiometries of the Phosphoenzyme and Total Phosphate Binding per Milligram of Protein

ligand[a]	amount of acid-stable EP	amount of total ^{32}P binding with ATP
MgATP	2.65 ± 0.14 ($n = 23$)	5.29 ± 0.17 ($n = 3$)
Mg-P_i	4.53 ± 1.41 ($n = 8$)	
CDTA-ATP		5.15 ± 0.14 ($n = 5$)

[a] Concentrations of MgATP, Mg-P_i, and CDTA-ATP are as described in Materials and Methods. [γ-^{32}P]ATP (0.1 mM) and $^{32}P_i$ (4 mM) for acid-stable EP, 0.4 mM [γ-^{32}P]ATP for the total amount of radioactive ^{32}P bound, and 5 or 10 mM CDTA were used.

acid (1 mCi) was diluted to 2 mL of 0.1 M phosphoric acid/Tris (pH 7.0) to provide a radioactivity of 0.5 mCi/mL. All other reagents were analytical grade or better.

RESULTS

Stoichiometry of Acid-Stable or Acid-Labile Radioactive Enzyme from ATP and P_i. The total amount of binding of labeled ^{32}P to the enzyme consists of both acid-stable phosphoenzyme ($E^{32}P$) and the acid-labile ATP complex (E·[γ-^{32}P]ATP). Table 1 summarizes the experiments in which either maximal binding of acid-stable phospoenzyme or the total amount of radioactive ATP was measured. As shown in the first line of Table 1, the gastric H,K-ATPase formed 2.7 ± 0.1 nmol of acid-stable phosphoenzyme per milligram of protein and 5.3 ± 0.2 nmol of total ^{32}P (acid-stable $E^{32}P$ + [γ-^{32}P]ATP) bound per milligram of protein (Table 1); 2.7 nmol of bound radioactivity was acid-stable EP generated from the high-ATP affinity binding site, and the other 2.6 nmol of radioactivity bound was due to binding of [γ-^{32}P]-ATP at a low-ATP affinity binding site without phosphorylation. A high concentration of ATP (>0.4 mM) was necessary to maintain maximum acid-labile radioactive binding to this half of the oligomeric enzyme as an E·ATP complex. Incubation with Mg-$^{32}P_i$ resulted in 4.5 nmol of radioactive P_i bound per milligram of protein as shown in line 2 of Table 1. The rate of formation of acid-stable phosphoenzyme from Mg-P_i was slower than that from MgATP. In the presence of CDTA, where no phosphorylation is possible, the preparation bound 5.15 nmol of ATP/mg of protein as shown in the bottom line of Table 1.

Characteristics of the Inhibition of Gastric H,K-ATPase Activity by INT. Imidazo[1,2-α]pyridine derivatives have been shown to be strictly K^+-competitive inhibitors of the gastric H,K-ATPase (*23*). A typical K^+-competitive inhibitor belonging to the imidazo[1,2-α]pyridine class is SCH28080, 3-(cyanomethyl)-2-methyl-8-(phenylmethoxy)imidazo[1,2-α]-pyridine (SCH28080) (*33*−*36*). Later, several fused ring analogues of SCH28080, for example, (2-methyl-8-phenyl-7,8-dihydro-6*H*-9-oxa-1,3a-diazacyclopenta[*a*]naphthalen-3-yl)acetonitrile and an imidazonaphthyridine derivative (INT), were synthesized that have a structure designed to mimic the known binding conformation of SCH28080 where the benzene ring is orthogonal to the imidazopyridine (Figure 1) (*27*, *28*, *37*, *38*). The binding properties of INT were investigated further.

The imidazonaphthyridine, INT, inhibits the gastric H,K-ATPase activity with an IC_{50} of 35 nM in the presence of 10 mM KCl and an IC_{50} of 24 nM in the presence of 2 mM KCl. The mechanism of inhibition was investigated by measuring the effect of the inhibitor on the H,K-ATPase activity in the presence of various concentrations of K^+. As shown in Figure 2, the inhibition by INT was K^+-competitive, since the INT increased the observed K_m value for K^+ with virtually no effect on the observed V_{max}. The K_i of INT of 47 nM was similar to the K_i of 56 nM found previously for SCH28080 (*23*).

Binding of INT to the H,K-ATPase in the Presence of MgATP. When 0.1 μM INT was incubated with the enzyme in the presence of MgATP, a B_{max} of 2.2 ± 0.09 nmol/mg of protein was obtained at 20 °C. The rate of INT binding was temperature-dependent (Figure 3A). The binding rate for INT was much slower at 1 °C ($t_{1/2} = 403$ s) compared to the rate obtained at 20 °C ($t_{1/2} = 135$ s). It has been shown previously that SCH28080 binds with a $t_{1/2}$ of 232 s at 1.5 °C and a $t_{1/2}$ of 5.4 s at 37 °C (*39*).

Binding of [^{3}H]INT was saturable at room temperature (Figure 3B). The maximal binding level (B_{max}) was 2.7 ± 0.1 nmol/mg of protein. The K_d was 30.9 ± 3.6 nM. This K_d is similar to that of SCH28080 ($K_d = 45$ nM) found previously (*39*). In these experiments, the level of INT binding per milligram of protein was constant up to a concentration of 1 μM. This stoichiometry is therefore the maximum for binding to the ATPase, and thus, only one site of the $(\alpha\beta)_2$ oligomer binds the inhibitor. The quantity of INT bound did not change with a varying concentration of Mg^{2+}, between 0.2 and 2 mM. Subsequent CDTA

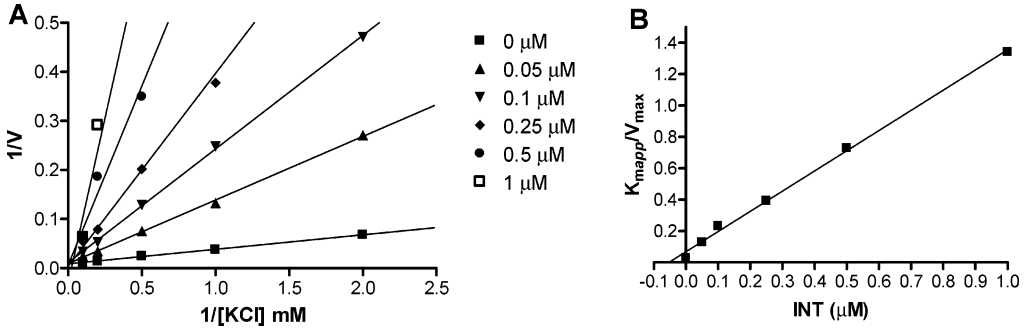

FIGURE 2: K^+-competitive inhibition of the gastric H,K-ATPase activity by INT. (A) Lineweaver−Burk plot showing strictly K^+-competitive inhibition kinetics in the presence of nigericin as described in Materials and Methods. The K^+-stimulated ATPase activity of the gastric vesicles was determined at 37 °C in the presence of increasing concentrations of the inhibitor at various concentrations of KCl. The gastric vesicles (2 μg/mL) were resuspended in a buffer composed of 20 mM Tris/HCl (pH 7.0), 2 mM $MgCl_2$, KCl (0−10 mM), nigericin (1 μg/mL), and either 0.05 (▲), 0.1 (▼), 0.25 (◆), 0.5 (●), and 1.0 μM (□) INT, or in the absence of the inhibitor (■). Values shown are means and ranges from triplicate determinations of the enzyme activity. (B) Secondary plot of the linear relationship between $K_{m(app)}/V_{max}$ and the inhibitor concentration. A K_m of 2.17 mM and a K_i 47 nM were calculated from this plot.

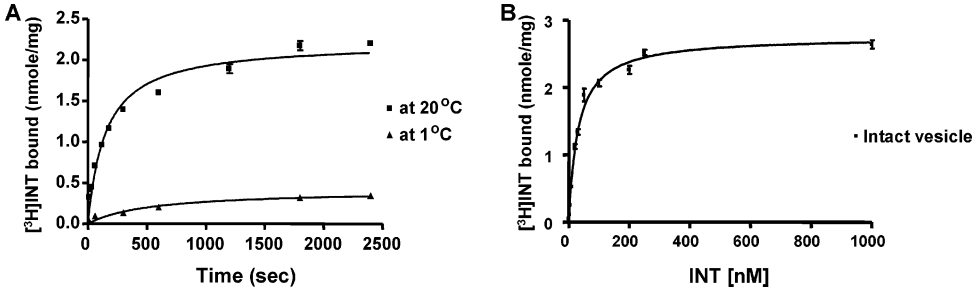

FIGURE 3: Temperature effects on INT binding and binding of INT in the presence of 2 mM MgATP. (A) Gastric vesicles (0.01 mg/mL) were incubated in a buffer composed of 20 mM Tris/HCl (pH 7.0), 2 mM $MgCl_2$, 2 mM ATP (pH 7.0, adjusted with Tris), and nigericin (2 μg/mL) in the presence of 0.1 μM [^{3}H]INT at 20 or 1 °C, and the amount of INT bound to the enzyme was determined as described in Materials and Methods. A B_{max} of 2.22 $\pm$ 0.088 nmol/mg of protein was obtained at 20 °C, and 0.39 $\pm$ 0.08 nmol/mg of protein was found at 1 °C. (B) Gastric vesicles (0.02 mg/mL) were incubated in a buffer composed of 20 mM Tris/HCl (pH 7.0), 2 mM $MgCl_2$, and 2 mM ATP (pH 7.0, adjusted with Tris) in the presence of increasing concentrations of [^{3}H]INT (from 0.1 nM to 1 μM) at 20 °C for 30 min, and the amount of INT bound to the enzyme was determined as described in Materials and Methods. The curve for intact vesicles represents binding of INT to the enzyme in the absence of nigericin. The calculated B_{max} was 2.72 $\pm$ 0.10 nmol/mg of protein for the intact vesicles. Each point is the average of three experiments. The presence of nigericin had no effect on INT binding.

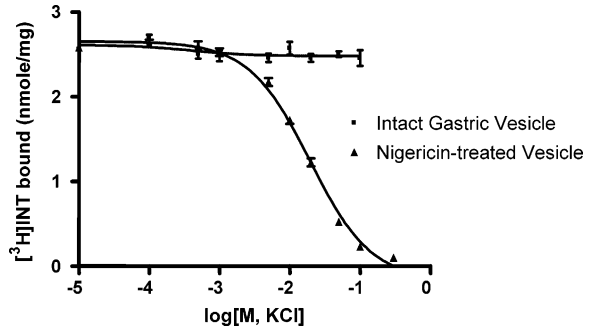

FIGURE 4: Displacement of INT binding by luminal K^+. INT binding was assessed at 20 °C in the presence of 2 mM MgATP. The intact gastric vesicle curve represents the incubation in the absence of nigericin, and the nigericin-treated vesicle curve represents the incubation in the presence of nigericin. The enzyme (10 μg/mL) was incubated in a buffer composed of 20 mM Tris/HCl (pH 7.0), 2 mM $MgCl_2$, 2 mM ATP, with or without 5 μg of nigericin/mL and 230 nM [^{3}H]INT, and KCl (0.001−300 mM). No effect of KCl addition was seen in this experiment in the absence of nigericin. In contrast, in the presence of nigericin, a $K_{m(app)}$ of 30.7 mM KCl in the presence of 230 nM INT was observed. Each measurement is the average of three experiments.

treatment to chelate Mg^{2+} did not reverse INT binding.

KCl did not displace INT binding in intact vesicles. However, in the presence of nigericin, KCl displaced INT, since in the presence of this ionophore K^+ was able to reach the luminal surface of the enzyme, the apparent location of the inhibitor binding site. These data are shown in Figure 4. There was a concentration-dependent displacement of INT binding by K^+ in the presence of nigericin. $K_{m(app)}$ was 5.2 mM at 18 nM INT and 30.7 mM at 230 nM INT. The $K_{m(app)}$ of KCl increased as the concentration of the inhibitor increased. This shows that binding of INT occurs in the region of the luminal K^+ binding site as previously found for SCH28080 (*24*, *39*).

Effects of Ligand on INT Binding. INT binding was also assessed in the presence of various ligands (Table 2 and Figure 5A). The maximal level of binding of INT was readily obtained in the presence of MgATP or Mg-P_i with a similar stoichiometry for inhibitor binding. Although the binding was slow in the presence of Mg^{2+} alone or Mg-vanadate, the binding of inhibitor eventually saturated with the same B_{max} as in the presence of MgATP. For example, at a concentration of 2 μM INT, 2.6−2.7 nmol of INT was bound per milligram

Table 2: Binding of INT (nmol/mg of protein)

ligand[a]	INT (0.1 μM)[b]	INT (2 μM)[b]
MgATP	2.36 $\pm$ 0.13 (n = 12)	2.64 $\pm$ 0.09 (n = 7)
Mg-P_i	2.18 $\pm$ 0.09 (n = 6)	2.64 $\pm$ 0.12 (n = 4)
Mg	0.89 $\pm$ 0.08 (n = 6)	2.63 $\pm$ 0.07 (n = 4)
Mg-vanadate	1.30 $\pm$ 0.01 (n = 3)	2.67 $\pm$ 0.05 (n = 4)
CDTA-ATP	0.28 $\pm$ 0.25 (n = 9)	0.52 $\pm$ 0.03 (n = 4)

[a] Concentrations of MgATP, Mg-P_i, Mg, Mg-vanadate, and CDTA-ATP are as described in Materials and Methods, namely, 2 mM Mg^{2+}, 0.1−2 mM ATP for INT binding, 4 mM P_i, 0.2 mM vanadate, and 5 or 10 mM CDTA. [b] INT binding was assessed after incubation at 20 °C for 30 min.

of the enzyme in the presence of either MgATP, Mg-P_i, Mg only, or Mg-vanadate after a 30 min incubation (Table 2). Similar data are found for SCH28080 binding. Although it has been shown that the B_{max} of SCH28080 was the same in the presence of either MgATP or Mg^{2+}, a 10-fold lower affinity of SCH28080 was observed in the presence of Mg^{2+} alone, compared to the affinity in the presence of MgATP (*39*). Binding of INT to CDTA-treated enzyme was observed to be only 10% of the maximal INT binding in the presence of Mg^{2+} as shown in Table 2 and Figure 5. This shows that Mg^{2+} is required for INT binding.

Relative Stoichiometry of Inhibitor and Acid-Stable Phosphoenzyme. The stoichiometry of INT binding was compared with that of the phosphoenzyme generated by ATP and shown to be 1:1. Maximal binding of INT was achieved after a 30 min incubation with 2 μM INT in the presence of Mg^{2+}; 2.6 nmol of INT was bound, and 2.6 nmol of acid-stable phosphoenzyme was formed per milligram of protein at high ATP concentrations (Tables 1 and 2), and hence, each oligomer has two binding sites, one for the inhibitor and one for phosphate.

The level of binding of inhibitor to the enzyme after an only 10 s incubation was ~0.3 $\pm$ 0.01 nmol of INT/mg of the enzyme (n = 3), as compared to the saturation binding, 2.6 $\pm$ 0.1 nmol of INT/mg protein after a 30 min incubation. Hence, binding is relatively slow.

High concentrations of ATP (0.1 mM) provided maximal acid-stable phosphoenzyme formation within 1 min using INT-bound enzyme. The total amounts of ^{32}P binding of INT-bound enzyme and native enzyme at high ATP concentrations were 4.5 $\pm$ 0.58 and 5.3 $\pm$ 0.17 nmol/mg of protein,

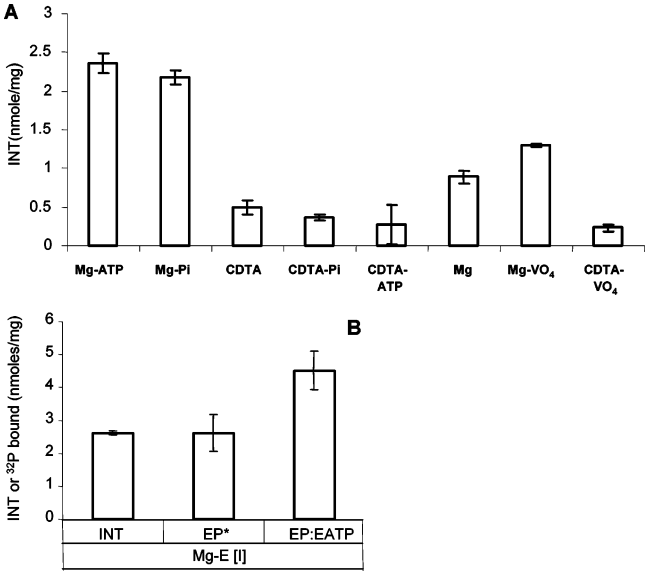

FIGURE 5: Effects of the ligand on the INT binding and acid-stable phosphoenzyme formation and total ^{32}P binding of the INT-bound enzyme. (A) The enzyme was incubated at 20 °C for 30 min as described in Materials and Methods with 0.1 μM [^{3}H]INT. MgATP, Mg-P_i, CDTA, CDTA-P_i, CDTA-ATP, Mg, Mg-VO_4, and CDTA-VO_4 represent INT binding in the presence of 2 mM MgATP, 2 mM $MgCl_2$ and 5 mM phosphate, 5 mM CDTA, 5 mM CDTA and 5 mM phosphate, 5 mM CDTA and 2 mM ATP, 2 mM $MgCl_2$, 2 mM $MgCl_2$ and 0.2 mM vanadate, and 5 mM CDTA and 0.2 mM vanadate, respectively. (B) Mg-E[I] means that results were obtained with INT-bound enzyme after incubation for 1 h in the absence of ATP but in the presence of Mg^{2+}. The enzyme (0.1 mg/mL) was incubated in a buffer composed of 2 μM [^{3}H]INT, with or without 2 mM $MgCl_2$ and 10 mM CDTA, and 20 mM Tris/HCl (pH 7.0) at 20 °C. Nonselective binding of INT was assessed by the pretreatment with nonlabeled 0.2 mM INT as described in Materials and Methods. When the INT-bound enzyme was treated with 0.1 mM [γ-^{32}P]ATP, 2.63 $\pm$ 0.57 nmol of acid-stable EP·(INT) was formed (represented by EP*, $n = 6$). The total nanomoles of ^{32}P bound to the INT-bound enzyme represented by EP:EATP was 4.52 $\pm$ 0.58 nmol/mg of protein ($n = 4$), which was prepared by an incubation in the presence of 0.4 mM [γ-^{32}P]-ATP.

respectively (Figure 5B and Table 1). This suggests that the inhibitor-bound enzyme also forms one acid-stable EP and one acid-labile E[ATP] on each half of the oligomer, as in the untreated enzyme at high ATP concentrations.

Enzyme Dephosphorylation in Nigericin-Treated Vesicles in the Presence of K$^+$. In the first set of experiments, only 10 μM ATP was used, to minimize re-formation of EP from radioactive ATP after K^+-dependent dephosphorylation. Dephosphorylation of the phosphoenzyme consists of spontaneous dephosphorylation of the E_2P·Mg^{2+} form (shown as Control in Figure 6) and K^+-stimulated dephosphorylation (shown with 10 mM KCl in Figure 6A). Spontaneous dephosphorylation of E_2P·Mg^{2+} is very slow as compared to dephosphorylation in the presence of K^+ (*11*, *13*, *15*, *25*, *40*). K^+ dephosphorylated ~88% of phosphoenzyme rapidly, and this fraction reflects the amount of the E_2P conformation (*25*). Approximately 12% of the phosphoenzyme was K^+-insensitive, probably E_1P. It was observed that INT increases the level of Mg^{2+}-dependent dephosphorylation very slightly (shown as 10 μM INT in Figure 6A). However, INT mainly increases the fraction of K^+-insensitive phosphoenzyme (compared to that obtained in the presence of K^+ ion only) (Figure 6), as shown previously for SCH28080 (*25*).

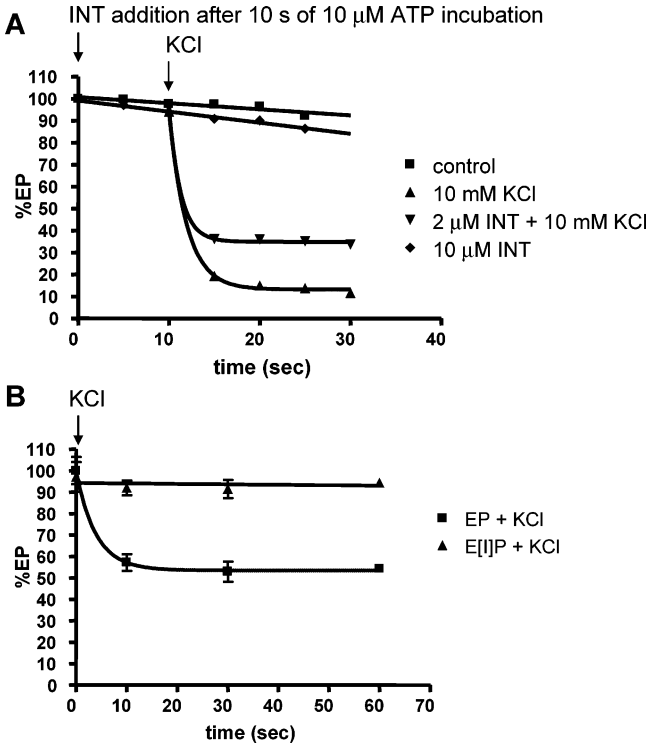

FIGURE 6: Effect of INT on K^+-stimulated dephosphorylation and effects of K^+ addition on native enzyme and on INT-bound enzyme. (A) Prior to addition of INT, the enzyme was incubated for 10 s with 10 μM [γ-^{32}P]ATP in the presence of nigericin, to form acid-stable EP. The phosphoenzyme formed by 10 μM [γ-^{32}P]ATP after a 10 s incubation at 20 °C represents 100% EP in this experiment. This was 1.74 nmol of EP/mg of protein after this short incubation time. After addition of INT, the enzyme suspension was incubated for 10 s at 20 °C and then 10 mM KCl was added (indicated by arrow). An aliquot was taken at timed intervals (15, 20, 25, and 30 s), and the phosphoenzyme level was measured and is represented as percentage of the EP formed before any additions. The control line represents EP levels in the absence of KCl or inhibitor; 10 μM INT represents the % EP formed in the presence of 10 μM INT but in the absence of KCl. The level is the same, showing a lack of an effect of INT on phosphorylation in this short incubation period. The dephosphorylation by 10 mM KCl for up to 30 s is also shown after the ATP incubation in the absence of INT, showing almost complete dephosphorylation. The line with 2 μM INT and 10 mM KCl represents the phosphoenzyme level obtained after INT addition 10 s after the 10 s ATP incubation followed by addition of 10 mM KCl after ATP incubation for 20 s. After KCl was added, the phosphoenzyme dephosphorylated rapidly. The phosphoenzyme formed at 10 μM ATP was 88% E_2P, which was K^+-sensitive. INT (2 μM) was able to inhibit a fraction of K^+-stimulated dephosphorylation of EP by competing with K^+. (B) The line with EP and KCl represents the phosphoenzyme level of the native enzyme in the presence of KCl, and the line with E[I]P and KCl represents the phosphoenzyme level of the INT-bound enzyme in the presence of KCl. Untreated or INT-treated gastric vesicles were resuspended in a buffer composed of 20 mM Tris/HCl (pH 7.0), 2 mM $MgCl_2$, 5 μg of nigericin/mL, and 0.1 mM [^{32}P]ATP/Tris (pH 7.0) at a protein concentration of 100 μg/mL for 60 s to give the maximal amount of acid-stable EP. KCl (5 mM) was added to the reaction mixture, and an aliquot was taken to measure the acid-stable EP level at timed intervals. The 100% EP level is that found after ATP incubation of the native enzyme for 60 s before KCl addition. The top curve shows that the acid-stable phosphoenzyme formed in the INT-bound enzyme is K^+-insensitive. The bottom curve shows the steady-state level of the phosphoenzyme formed at these high ATP concentrations due to rephosphorylation of the enzyme during the incubation period. Approximately half of the phosphoenzyme formed at high ATP concentrations was K^+-insensitive.

In the second set of experiments, the effect of addition of K^+ to the acid-stable phosphoenzyme formed from INT-bound enzyme at high ATP concentrations (>0.1 mM) was investigated. The level of phosphoenzyme formation by INT-bound enzyme was 97% of maximal EP of the native enzyme in this particular set of experimental condition. In contrast to the major conformation of the acid-stable phosphoenzyme generated at low ATP concentrations that was K^+-sensitive E_2P, only 3% of the enzyme was dephosphorylated by K^+ addition, showing that the major phosphoenzyme conformation of INT-bound enzyme here was the K^+-insensitive E_1P, not the E_2P conformation. The phosphoenzyme formed at high ATP concentrations showed ~50% of K^+-insensitive E_1P by continuous phosphorylation, representing a 1:1 mixture of E_1P:E_2[ATP] and E_2P:E_1[ATP] (Figures 5B and 6B).

DISCUSSION

The P_2-type ATPases represent a diverse family of cation transporters that share structural and kinetic characteristics (*41*, *42*). Crystallization of one member of the family, the SR Ca-ATPase, has revealed the likely general three-dimensional structure of the various members of this family, including the gastric H,K-ATPase and Na,K-ATPase. Since electrophoresis and cross-linking studies (*18*) had suggested the gastric H,K-ATPase of the parietal cell might exist as a dimeric heterodimer, here we have performed studies to determine the possible functional consequences of this oligomeric form. The results of these studies clearly demonstrate that the fully functional enzyme is present in the oligomer, but the properties of each subunit are distinctive as shown by either phosphorylation, ATP binding, or inhibitor binding and its effects. Given the structural similarities among these pumps, it is possible that, at least, the other heterodimeric P_2-type ATPase, the Na,K-ATPase, also acts functionally as an oligomer.

In the dimeric oligomer of the H,K-ATPase, each half was able to act independently, suggesting that the enzyme is fully active and there are no deleterious consequences of the oligomeric form but that the properties of the oligomer could result in functional interactions between the subunits. In the data presented above, there is reasonable evidence that, whereas fully functional protein is present in the oligomer, the properties of each subunit are distinctive as shown by either phosphorylation, ATP binding, or inhibitor binding and its effects.

General Evidence that the Quaternary Structure Form of the ATPase Is an Oligomer. Structurally, the gastric H,K-ATPase appears to exist as a dimeric heterodimer in isolated gastric membranes, $(\alpha\beta)_2$ (*18*). Thus, Blue Native gel electrophoresis of the *n*-dodecyl β-D-maltoside-solubilized enzyme showed that a majority of the enzyme is a dimeric heterodimer, $(\alpha\beta)_2$, with a minor band corresponding to a tetrameric heterodimer, $(\alpha\beta)_4$, both with native and with expressed enzyme (*18*, *43*, *44*). Also, using high-performance gel chromatography and total internal reflection fluorescence microscopy, both a diprotomer, $(\alpha\beta)_2$, and a tetraprotomer, $(\alpha\beta)_4$, were detected in nonionic detergent-solubilized enzyme (*45*).

Cross-linking by Cu^{2+}-phenanthroline resulted in formation of an $(\alpha\beta)_2$ oligomer. Cleavage analysis showed that a fragment beginning at Val^{561} and ending at Arg^{616} is likely to be the region of closest contact between two α subunits (*18*). This region is in the N domain of the enzyme that undergoes significant oscillatory conformational changes during the transport cycle (*46*), and these may determine an out-of-phase conformation during catalysis. In the Na,K-ATPase, the dimerizing domain localized to the C-terminal side of Ala^{439} was shown by Cu^{2+}-phenanthroline cross-linking (*47*), which was narrowed to Gly^{554}−Pro^{785} by chimeric analysis (*4*).

The results of studies on ATP-dependent Ca^{2+} binding also provided evidence for a functional effect of an oligomeric structure; 1.2 mol of Ca^{2+} molecules bound to one molecule of acid-stable phosphoenzyme at 10 μM ATP, but 2.2 mol of Ca^{2+} bound to one molecule of acid-stable phosphoenzyme at 1000 μM ATP (*48*, *49*). These data can be interpreted as showing that $E_2P\cdot Ca:E_1$ is present at low ATP concentrations and $E_2P\cdot Ca:E_1$[ATP]·Ca is formed at high ATP concentrations. Thus, the binding properties for the divalent cation also suggest a dimeric oligomer is the structure of the H,K-ATPase.

Phosphoenzyme Stoichiometry as Evidence for a Functional Oligomer. The stoichiometry of phosphorylation of the various P_2-type ATPases has been a subject of controversy. For example, the Na,K-ATPase has been shown to consist of two possible forms with a maximum of 0.5 mol of ADP-sensitive phosphoenzyme (NaE_1P) or 0.5 mol of potassium-sensitive phosphoenzyme (E_2P) (*50*). However, phosphorylation at a low-affinity site of SDS-purified Na,K-ATPase (*51*) and fluorescence resonance energy transfer studies using ouabain modified with different fluorescent probes (*52*) show that the monomeric heterodimer ($\alpha\beta$) of the enzyme is fully active. The Na,K-ATPase of the nasal salt gland of the duck bound 3.6 nmol of ouabain/mg of protein with 7.0 nmol of phosphoenzyme/mg formed with ATP (*53*) or 5.9 nmol of phosphoenzyme/mg of protein formed with Mg-P_i (*54*). This showed full site reactivity with phosphorylation but only half-site reactivity with the inhibitor. Another report showed that pig renal enzyme provided a stoichiometry of 0.5:1:1 for phosphate from ATP, ouabain, and ATP (*55*) therefore, with half-site reaction with ATP phosphorylation and full site reactivity with inhibitor. Digestion of the Na,K-ATPase by chymotrypsin resulted in an increase in the amount of acid-stable EP from 0.5 to 1 mol/mol enzyme, also suggesting half-site reactivity of the unmodified ATPase (*56*). Expression of the Na,K-ATPase in insect cells showed that an oligomer of this enzyme was formed in this heterologous expression system during biosynthesis in the endoplasmic reticulum, indicating that there is a natural tendency for this heterodimeric P_2-type ATPase to form an oligomer (*2*). Similarly, nondenaturing gels of the H,K-ATPase expressed in mammalian cells show the presence of an oligomeric form of the enzyme (*43*, *44*).

Studies on the Ca-ATPase showed that whereas 0.5 mol of phosphoenzyme/mol of enzyme was generated by ATP, the maximum phosphoenzyme level obtained by UTP or Mg-P_i was 1 mol of EP/mol of enzyme (*57*). The apparent half-site reactivity, as for the SR Ca-ATPase, appears to be dependent on the nature of the phosphorylating substrate since UTP resulted in full site reactivity but ATP in only half-site reactivity (*57*, *58*). This may be due to the smaller size of UTP versus ATP. These results were interpreted as

showing the presence of an E_1:E_2 dimer when ATP was the phosphorylating substrate.

In the case of the gastric H,K-ATPase, different stoichiometries of acid-stable phosphoenzyme have been reported, especially when low concentrations of ATP, such as 5−10 μM, were used. This approach has not generally taken into account the reduction of ATP concentrations due to enzyme hydrolysis and hence the loss of phosphorylating substrate. The stoichiometry of acid-stable phosphoenzyme per milligram of the gastric H,K-ATPase has thus been variously stated to be 0.6−0.69 (*26*), 1.0−1.2 (*25*, *59*), 1.3−1.5 (*11*, *13*), and 2.4−2.7 nmol (*19*, *60*).

We observed formation of 1.3 nmol of acid-stable phosphoenzyme/mg of protein at 0−1 °C (data not shown), similar to that reported previously at this temperature (*25*). However, at 20 °C, 2.6−2.7 nmol of acid-stable phosphoenzyme per milligram of protein was formed in the presence of 0.1 mM ATP over a 10 min period as described previously (*19*). Thus, low concentrations of ATP (<10 μM) produced only acid-stable phosphoenzyme from the high-ATP affinity site since the $K_{m(app)}$ of high ATP affinity is 1.1 μM.

The $K_{m(app)}$ of the low-affinity site is 0.12−0.15 mM (*19*, *45*), and this is presumably the affinity for the acid-labile binding of ATP which will occur at the ∼3 mM ATP levels known to be present in the parietal cell (*61*). In the absence of divalent ions such as Mg^{2+} and Ca^{2+}, ATP can bind to the enzyme to form a E[ATP] complex without forming phosphoenzyme (*11, 15*). The total amount of binding of ATP as an E[ATP] complex was found to be 5.2 nmol/ mg of protein, which is twice the level of acid-stable phosphoenzyme, EP. High concentrations of ATP (>0.4 mM) provided maximal acid-stable EP and acid-labile binding of ^{32}P to the enzyme as an E[ATP] complex. The relative stoichiometry of EP:E[ATP] in the H,K-ATPase with Mg^{2+} in our experiments was 1: 1 to give the total of 5.2 nmol of radioactivity bound with [γ^{32}-P]ATP. The stoichiometry of acid-stable EP from acetyl phosphate has been shown to be 4.2 nmol/mg of protein (*60*), and we obtained a similar value for phosphorylation from inorganic phosphate. This may be due to the small size of the phosphorylating substrate as compared to ATP and less interference of the nucleotide binding domain between the two $\alpha\beta$ oligomers.

Various detergents were tried on the gastric H,K-ATPase to see if acid-stable EP could be increased by dissociation of the oligomer. However, treatment with nonionic detergents such as $C_{12}E_8$ reduced the level of EP formation. For example, treatment with 0.01 and 0.1% $C_{12}E_8$ resulted in only 1.2 and 0.33 nmol of EP/mg of the enzyme, respectively (J. M. Shin, unpublished data). Treatment with 0.6% $C_{12}E_8$ has been previously reported to result in formation of only 0.11 nmol of EP/mg (*45*). These data show that disruption of the oligomeric structure of the H,K-ATPase, at least with this detergent, does not increase but inhibits EP formation. Treatment with low concentrations of SDS such as is done for purification of the Na,K-ATPase did not increase the amount of acid-stable EP (*19*).

The nature of the phosphoenzyme conformation was different depending on the ATP concentration. The phosphoenzyme generated at low ATP concentrations consisted of ∼90% K^+-sensitive E_2P and 10% K^+-insensitive E_1P, without acid-labile ATP binding; however, high ATP concentrations provided an ∼1:1 mixture of K^+-sensitive E_2P:E_1[ATP] and K^+-insensitive E_1P:E_2[ATP].

Inhibitor Binding and Functional Effects Consistent with a Dimeric Oligomer. INT (2.6 nmol) bound to the enzyme in the presence of MgATP with full inhibition of enzyme activity. Thus, binding at half the ATP sites was sufficient to completely prevent enzyme turnover. This would be predicted from a dimeric functional oligomeric form of the enzyme.

INT-bound enzyme inhibited phosphorylation at low ATP concentrations, while the inhibitor-bound enzyme allows phosphorylation at high ATP concentrations. This is similar to data found for the SCH28080-bound enzyme. SCH28080 is known to have a higher apparent affinity for E_2P (*25*), but the stable form appears to be E_2[SCH28080] (*23*). Although SCH28080 inhibited the ATP phosphorylation at low ATP concentrations, the SCH28080-bound enzyme was phosphorylated at a high concentration of ATP or phosphate (*26*). Acid-labile ATP binding of SCH28080-bound enzyme has not been assessed at high ATP concentrations. Phosphorylation of INT-bound enzyme showed very slow formation of acid-stable phosphoenzyme at a low concentration of ATP; however, high concentrations of ATP resulted in maximal acid-stable phosphoenzyme and acid-labile ATP binding. One mole of the K^+-competitive inhibitor is bound per 2 mol of the enzyme, which now has 1 mol of acid-stable EP and 1 mol of the acid-labile ATP bound. The acid-stable phosphoenzyme in the inhibitor-bound conformation is K^+-insensitive, confirming that its conformation is E_1P, not the E_2P formed by the native enzyme at low ATP concentrations. Since the enzyme remains fully inhibited, the E_1P conformation cannot convert to the E_2P form in the presence of inhibitor since this would result in sensitivity of the phosphoenzyme to the addition of K^+.

The region of SCH28080 binding at the luminal surface of the enzyme consists of transmembrane segments, M4 (Ala^{335}), the M5−M6 loop (Leu^{809}), M6 (Cys^{813}), and M8 (Tyr^{922} and Ile^{940}) regions (*46*, *62*). Since the structure of INT mimics the active conformation of SCH28080, the INT binding site is likely to be at the SCH28080 binding site, which fixes this half of the oligomer in the E_2·(INT) form. The size of the K^+-competitive inhibitor may prevent conformational changes in the enzyme by limiting the movement of the liganded transmembrane segments, fixing the enzyme in the E_2P·(INT):E_1 or E_2·(INT):E_1 conformation. The distortion of the membrane binding region of INT appears to allow phosphorylation by ATP of the other heterodimer at high ATP concentrations.

Binding of Mg^{2+} to the enzyme is stable until the E_1 form is regenerated (*25*, *39*). Therefore, the E_2·INT conformation of the INT-bound enzyme appears to chelate Mg^{2+} in the enzyme P-domain in a region inaccessible to CDTA as shown previously for Ca^{2+} binding, in contrast to the Na,K-ATPase (*48*, *63*, *64*).

Since treatment with excess CDTA did not affect the inhibitor binding of the INT-bound enzyme, the conformation of the INT-bound enzyme is likely to be E_2·Mg·$(INT)_{exo}$:E_1·Mg with the Mg^{2+} binding in the E_2 form not accessible to CDTA, while the other fraction, E_1·Mg, remains accessible to CDTA since it was shown that CDTA can access Mg^{2+} in the E_1 conformation (*48*). High concentrations of ATP

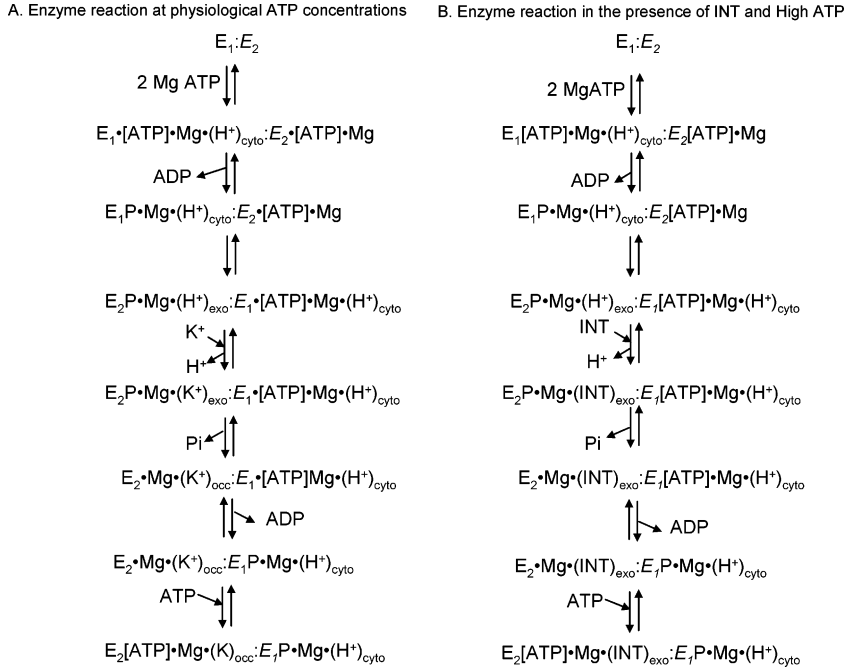

FIGURE 7: Postulated reaction profile scheme of the gastric H,K-ATPase oligomer at physiological ATP concentrations without and with inhibitor. The second oligomer is italicized for clarity. Panel A shows that at high ATP concentrations (>0.1 mM), ATP binds at high-ATP affinity binding sites to form the phosphoenzyme and additionally ATP binds to a low-ATP affinity binding site to form $E_1P{\cdot}Mg{\cdot}(H^+)_{cyto}$:$E_2$[ATP]·Mg, which converts to $E_2P{\cdot}Mg{\cdot}(H^+)_{exo}$:$E_1$[ATP]·Mg. In the presence of K^+, $E_2P{\cdot}Mg{\cdot}(K^+)_{exo}$:$E_1$[ATP]·$Mg{\cdot}(H^+)_{cyto}$ is formed and K^+-stimulated dephosphorylation results in a K^+-occluded $E_2{\cdot}Mg{\cdot}(K^+)_{occ}$:$E_1$[ATP]·$Mg{\cdot}(H^+)_{cyto}$. The E_1[ATP] part of the oligomer is phosphorylated to form $E_2{\cdot}Mg{\cdot}(K^+)_{occ}$:$E_1P{\cdot}Mg{\cdot}(H^+)_{cyto}$. This conformation can bind ATP at high ATP concentrations to form E_2[ATP]·$Mg{\cdot}(K^+)_{occ}$:$E_1P{\cdot}Mg{\cdot}(H^+)_{cyto}$. Panel B shows that INT competes with K^+ to form $E_2P{\cdot}Mg{\cdot}(INT)_{exo}$:$E_1$[ATP]·$Mg{\cdot}(H^+)_{cyto}$, which is dephosphorylated to $E_2{\cdot}Mg{\cdot}(INT)_{exo}$:$E_1$[ATP]·$Mg{\cdot}(H^+)_{cyto}$. The E_1[ATP] half of the dimer of this conformation can be phosphorylated to form $E_2{\cdot}Mg{\cdot}(INT)_{exo}$:$E_1P{\cdot}Mg{\cdot}(H^+)_{cyto}$, presumably because INT binding allows phosphate transfer. This phosphoenzyme form is K^+-insensitive. This conformation, however, can bind an additional ATP at the low-ATP affinity E_2 binding site to form E_2[ATP]·$Mg{\cdot}(INT)_{exo}$:$E_1P{\cdot}Mg{\cdot}(H^+)_{cyto}$.

provided the maximal quantity of both acid-stable phosphoenzyme and acid-labile ATP binding.

A Reaction Scheme for the H,K-ATPase Incorporating the Oligomer Effects. A proposed scheme of the gastric H,K-ATPase reaction based on the different stoichiometries found here is shown in Figure 7. The left panel and right panel show the reaction steps in the absence of inhibitor and in the presence of inhibitor, respectively. Since 10 μM ATP in the presence of Mg^{2+} forms only acid-stable phosphoenzyme, without forming an acid-labile E[ATP] complex, the initial conformation after phosphorylation at low ATP concentrations is probably $E_1P{\cdot}Mg(H^+_{cyto})$:$E_2{\cdot}Mg$ that converts to $E_2P{\cdot}Mg{\cdot}(H^+)_{exo}$:$E_1{\cdot}Mg{\cdot}(H^+)$ followed by proton release and formation of the K^+-sensitive E_2P conformation, $E_2P{\cdot}Mg{\cdot}(K^+)$:$E_1{\cdot}Mg{\cdot}(H^+)$, that dephosphorylates to $E_2K{\cdot}Mg$:$E_1{\cdot}Mg{\cdot}(H^+)$ (*11*, *13*, *40*). However, higher concentrations of MgATP (>0.1 mM) result in the formation of ~50% K^+-sensitive E_2P:E_1[ATP] and 50% K^+-insensitive E_1P:E_2[ATP] by continuous rephosphorylation, explaining the higher total ^{32}P binding stoichiometry at high ATP concentrations. In the presence of INT-inhibited enzyme at high ATP concentrations, ATP can phosphorylate the enzyme to form a K^+-insensitive acid-stable EP and can also form the E_2(INT)-[ATP] by binding at the ATP binding site in the N-domain even though this is in the E_2 conformation as shown in Figures 5B and 6B.

The conformation of the INT-bound enzyme at high ATP concentrations is likely initially to be E_2[ATP]·$Mg{\cdot}(INT)_{exo}$:E_1[ATP]·$Mg{\cdot}(H^+)_{cyto}$ changing to E_2[ATP]·$Mg{\cdot}(INT)_{exo}$:$E_1P{\cdot}Mg{\cdot}(H^+)_{cyto}$. This reflects the INT reaction scheme of the oligomeric enzyme shown in Figure 7. MgATP at high concentrations forms $E_1P{\cdot}Mg$:E_2[ATP]·Mg followed by $E_2P{\cdot}Mg$:E_1[ATP]·Mg via a conformational change. INT binds to the E_2P half of the dimer to form $E_2P{\cdot}Mg{\cdot}(INT)_{exo}$:$E_1$-[ATP]·$Mg{\cdot}(H^+)_{cyto}$. This is dephosphorylated to $E_2{\cdot}Mg{\cdot}(INT)_{exo}$:$E_1$[ATP]·$Mg{\cdot}(H^+)_{cyto}$ following the phosphorylation of the E_1[ATP] half of the dimer to form a K^+-insensitive $E_2{\cdot}Mg{\cdot}(INT)_{exo}$:$E_1P{\cdot}Mg{\cdot}(H^+)_{cyto}$ conformation. This conformation, however, can bind an additional ATP at the low-ATP affinity E_2 binding site to form E_2[ATP]·$Mg{\cdot}(INT)_{exo}$:$E_1P{\cdot}Mg{\cdot}(H^+)_{cyto}$.

The demonstration that only half of the enzyme formed acid-stable phosphoenzyme while the other half of the enzyme bound ATP without phosphorylation or only half of the enzyme bound INT while the other half did not bind the inhibitor implies that the functional oligomeric enzyme in intact gastric vesicles allows only an E_1:E_2 conformation with two different ATP sites, one with high and one with low affinity (*45*). This conformation also results in two different Ca^{2+}-binding site affinities, dependent on ATP binding affinity (*49*). These inhibitory data for INT showing a stoichiometry of ~2.5 nmol/mg of enzyme also correlate with the covalent inhibition of the ATPase in vivo by proton pump inhibitors that have a similar stoichiometry (*65*).

These results give us further insight into the mechanism of action of these drugs: It is likely there is activation on the surface of one oligomer of the pump to form the thiophilic sulfenic acid followed by formation of a disulfide

at cysteine 813 mimicking an E_2 conformation. This process prevents activation on the other oligomer and results in full inhibition with half-of-site binding. These results would not be obtained if the activation mechanism occurred in free solution forming the sulfenamide with free access of the activated drug to both cysteines at position 813 as was once thought (*66*).

The contact region between two α subunits was shown to be a domain from Val^{561} to Arg^{616} (*18*) by Cu-phenanthroline cross-linking of the native enzyme. This implies that the maximum distance between these two regions is ~3 Å. This region crosses from a helix at the surface of the cytoplasmic region near the P-domain to the N-domain, based on the crystal structure of Ca-ATPase (*7*, *8*) and homology modeling of the H,K-ATPase (*46*). There are relatively large conformational changes in this region in transition from the ATP-liganded enzyme to the E_1P and then the E_2P form. It seems likely that the close association of the enzyme in its dimeric oligomeric form prevents at least the cytoplasmic domain, particularly the N-domain, from achieving identical open conformations like those that occur in the E_1 structure of the SR Ca-ATPase (*7*).

The benefits of this oligomeric structure of the H,K-ATPase are not clear. At the high concentration of ATP in the parietal cell, the second half of the oligomer will have ATP bound when in the E_1 conformation. This prevents the formation of E_1K^+ at the internal K^+ concentration of 150 mM which would inhibit enzyme turnover (*59*). Hence, this half of the oligomer can rapidly convert to the transport conformation: the ATP-bound E_1 form being converted to E_1P and then E_2P with release of a proton, without the delay due to the ATP-dependent release of K^+ from the E_1K^+ formed from the other half of the oligomer that has derived from the dephosphorylation of E_2P.

Thus, perhaps the oligomeric structure of this enzyme enables a more rapid turnover of the pump under physiological conditions. Alternatively, the out-of-phase conformation may be able to restrict back leak of H^+ at the very acidic pH of the active parietal cell that might occur if the oligomer formed $E_2P{\cdot}E_2P$. The structural explanation for this out-of-phase conformation may depend on the motion of the N- and A-domains of the enzyme during its catalytic cycle. Further, since all the P_2-type ATPases have structural homology and share kinetic characteristics, the detailed results obtained for the H,K-ATPase could have general implications for the other ATPases of this family.

ACKNOWLEDGMENT

We are grateful to Dr. Jeffery A. Kraut for a careful review of the paper.

REFERENCES

1. Taniguchi, K., Kaya, S., Abe, K., and Mardh, S. (2001) The oligomeric nature of Na/K-transport ATPase, *J. Biochem. 129*, 335−342.
2. Laughery, M., Todd, M., and Kaplan, J. H. (2004) Oligomerization of the Na,K-ATPase in cell membranes, *J. Biol. Chem. 279*, 36339−36348.
3. Kaya, S., Abe, K., Taniguchi, K., Yazawa, M., Katoh, T., Kikumoto, M., Oiwa, K., and Hayashi, Y. (2003) Oligomeric structure of P-type ATPases observed by single molecule detection technique, *Ann. N.Y. Acad. Sci. 986*, 278−280.
4. Koster, J. C., Blanco, G., and Mercer, R. W. (1995) A cytoplasmic region of the Na,K-ATPase α-subunit is necessary for specific α/α association, *J. Biol. Chem. 270*, 14332−14339.
5. Ovchinnikov, Yu. A., Demin, V. V., Barnakov, A. N., Kuzin, A. P., Lunev, A. V., Modyanov, N. N., and Dzhandzhugazyan, K. N. (1985) Three-dimensional structure of $(Na^+{+}K^+)$-ATPase revealed by electron microscopy of two-dimensional crystals, *FEBS Lett. 190*, 73−76.
6. Stein, W. D., Lieb, W. R., Karlish, S. J., and Eilam, Y. (1973) A modle for active transport of sodium and potassium ions as mediated by a tetrameric enzyme, *Proc. Natl. Acad. Sci. U.S.A. 70*, 275−278.
7. Toyoshima, C., Nakasako, M., Nomura, H., and Ogawa, H. (2000) Crystal structure of the calcium pump of sarcoplasmic reticulum at 2.6 Å resolution, *Nature 405*, 647−655.
8. Toyoshima, C., and Nomura, H. (2002) Structural changes in the calcium pump accompanying the dissociation of calcium, *Nature 418*, 605−611.
9. Hall, K., Perez, G., Anderson, D., Gutierrez, C., Munson, K., Hersey, S. J., Kaplan, J. H., and Sachs, G. (1990) Location of the carbohydrates present in the HK-ATPase vesicles isolated from hog gastric mucosa, *Biochemistry 29*, 701−706.
10. Geering, K. (1991) The functional role of the β-subunit in the maturation and intracellular transport of Na,K-ATPase, *FEBS Lett. 285*, 189−193.
11. Wallmark, B., Stewart, H. B., Rabon, E., Saccomani, G., and Sachs, G. (1980) The catalytic cycle of gastric $(H^+{+}K^+)$-ATPase, *J. Biol. Chem. 255*, 5313−5319.
12. Walderhaug, M. O., Post, R. L., Saccomani, G., Leonard, R. T., and Briskin, D. P. (1985) Structural relatedness of three ion-transport adenosine triphosphatases around their active sites of phosphorylation, *J. Biol. Chem. 260*, 3852−3859.
13. Stewart, B., Wallmark, B., and Sachs, G. (1981) The interaction of H^+ and K^+ with the partial reactions of gastric $(H^+{+}K^+)$-ATPase, *J. Biol. Chem. 256*, 2682−2690.
14. Wallmark, B., and Mardh, S. (1979) Phosphorylation and dephosphorylation kinetics of potassium-stimulated ATP phosphohydrolase from hog gastric mucosa, *J. Biol. Chem. 254*, 11899−11902.
15. Rabon, E., Sachs, G., Mardh, S., and Wallmark, B. (1982) ATP/ADP exchange activity of gastric $(H^+{+}K^+)$-ATPase, *Biochim. Biophys. Acta 688*, 515−524.
16. Rabon, E. C., Smillie, K., Seru, V., and Rabon, R. (1993) Rubidium occlusion within tryptic peptides of the H,K-ATPase, *J. Biol. Chem. 268*, 8012−8018.
17. Rabon, E., Wilke, M., Sachs, G., and Zampighi, G. (1986) Crystallization of the gastric H,K-ATPase, *J. Biol. Chem. 261*, 1434−1439.
18. Shin, J. M., and Sachs, G. (1996) Dimerization of the gastric H^+,K^+-ATPase, *J. Biol. Chem. 271*, 1904−1908.
19. Abe, K., Kaya, S., Imagawa, T., and Taniguchi, K. (2002) Gastric H/K-ATPase liberates two moles of P_i from one mole of phosphoenzyme formed from a high-affinity ATP binding site and one mole of enzyme-bound ATP at the low-affinity site during cross-talk between catalytic subunits, *Biochemistry 41*, 2438−2445.
20. Helmich-de Jong, M. L., van Emst-de Vries, S. E., Swarts, H. G., Schuurmans Stekhoven, F. M., and de Pont, J. J. (1986) Presence of a low-affinity nucleotide binding site on the $(K^+{+}H^+)$-ATPase phosphoenzyme, *Biochim. Biophys. Acta 860*, 641−649.
21. Chang, H., Saccomani, G., Rabon, E., Schackmann, R., and Sachs, G. (1977) Proton transport by gastric membrane vesicles, *Biochim. Biophys. Acta 464*, 313−327.
22. Ljungstrom, M., and Mardh, S. (1985) Kinetics of the acid pump in the stomach. Proton transport and hydrolysis of ATP and *p*-nitrophenyl phosphate by the gastric H,K-ATPase, *J. Biol. Chem. 260*, 5440−5444.
23. Wallmark, B., Briving, C., Fryklund, J., Munson, K., Jackson, R., Mendlein, J., Rabon, E., and Sachs, G. (1987) Inhibition of gastric H^+,K^+-ATPase and acid secretion by SCH 28080, a substituted pyridyl(1,2a)imidazole, *J. Biol. Chem. 262*, 2077−2084.
24. Keeling, D. J., Laing, S. M., and Senn-Bilfinger, J. (1988) SCH 28080 is a lumenally acting, K^+-site inhibitor of the gastric $(H^+{+}K^+)$-ATPase, *Biochem. Pharmacol. 37*, 2231−2236.
25. Mendlein, J., and Sachs, G. (1990) Interaction of a K^+-competitive inhibitor, a substituted imidazo[1,2a]pyridine, with the phospho- and dephosphoenzyme forms of H^+,K^+-ATPase, *J. Biol. Chem. 265*, 5030−5036.
26. Van der Hijden, H. T., Koster, H. P., Swarts, H. G., and De Pont, J. J. (1991) Phosphorylation of H^+/K^+-ATPase by inorganic

phosphate. The role of K^+ and SCH 28080, *Biochim. Biophys. Acta 1061*, 141−148.
27. Kaminski, J. J., Puchalski, C., Solomon, D. M., Rizvi, R. K., Conn, D. J., Elliott, A. J., Lovey, R. G., Guzik, H., Chiu, P. J., Long, J. F., and McPhail, A. T. (1989) Antiulcer agents. 4. Conformational considerations and the antiulcer activity of substituted imidazo-[1,2-a]pyridines and related analogues, *J. Med. Chem. 32*, 1686−1700.
28. Kaminski, J. J., Wallmark, B., Briving, C., and Andersson, B. M. (1991) Antiulcer agents. 5. Inhibition of gastric H^+/K^+-ATPase by substituted imidazo[1,2-a]pyridines and related analogues and its implication in modeling the high affinity potassium ion binding site of the gastric proton pump enzyme, *J. Med. Chem. 34*, 533−541.
29. Sachs, G., Chang, H. H., Rabon, E., Schackman, R., Lewin, M., and Saccomani, G. (1976) A nonelectrogenic H^+ pump in plasma membranes of hog stomach, *J. Biol. Chem. 251*, 7690−7698.
30. Rabon, E. C., Bin Im, W., and Sachs, G. (1988) Preparation of gastric H^+,K^+-ATPase, *Methods Enzymol. 157*, 649−654.
31. Yoda, A., and Hokin, L. E. (1970) On the reversibility of binding of cardiotonic steroids to a partially purified (Na+K)-activated adenosinetriphosphatase from beef brain, *Biochem. Biophys. Res. Commun. 40*, 880−886.
32. Lowry, O. H., Rosebrough, N. J., Farr, A. L., and Randall, R. J. (1951) Protein measurement with the Folin phenol reagent, *J. Biol. Chem. 193*, 265−275.
33. Kaminski, J. J., Hilbert, J. M., Pramanik, B. N., Solomon, D. M., Conn, D. J., Rizvi, R. K., Elliott, A. J., Guzik, H., Lovey, R. G., Domalski, M. S., Wong, S. C., Puchalski, C., Gold, E. H., Long, J. F., Chiu, P. J., and McPhail, A. T. (1987) Antiulcer agents. 2. Gastric antisecretory, cytoprotective, and metabolic properties of substituted imidazo[1,2-a]pyridines and analogues, *J. Med. Chem. 30*, 2031−2046.
34. Bristol, J. A., and Puchalski, C. (1984) Imidazo[1,2-a]pyridines and use, U.S. Patent 4,450,164.
35. Kaminski, J. J., Bristol, J. A., Puchalski, C., Lovey, R. G., Elliott, A. J., Guzik, H., Solomon, D. M., Conn, D. J., Domalski, M. S., Wong, S. C., Gold, E. H., Long, J. F., Chiu, P. J., Steinberg, M., and McPhail, A. T. (1985) Antiulcer agents. 1. Gastric antisecretory and cytoprotective properties of substituted imidazo[1,2-a]-pyridines, *J. Med. Chem. 28*, 876−892.
36. Kaminski, J. J., Perkins, D. G., Frantz, J. D., Solomon, D. M., Elliott, A. J., Chiu, P. J., and Long, J. F. (1987) Antiulcer agents. 3. Structure−activity-toxicity relationships of substituted imidazo-[1,2-a]pyridines and a related imidazo[1,2-a]pyrazine, *J. Med. Chem. 30*, 2047−2051.
37. Gold, E. H., Kaminski, J. J., and Puchalski, C. (1984) Antiulcer tricyclic imidazo[1,2-a]pyridines, U.S. Patent 4,468,400.
38. Senn-Bilfinger, J. (2002) Imidazonaphthyridines, U.S. Patent 6,384,048 B1.
39. Keeling, D. J., Taylor, A. G., and Schudt, C. (1989) The binding of a K^+ competitive ligand, 2-methyl,8-(phenylmethoxy)imidazo-(1,2-a)pyridine 3-acetonitrile, to the gastric (H^++K^+)-ATPase, *J. Biol. Chem. 264*, 5545−5551.
40. Brzezinski, P., Malmstrom, B. G., Lorentzon, P., and Wallmark, B. (1988) The catalytic mechanism of gastric H^+/K^+-ATPase: Simulations of pre-steady-state and steady-state kinetic results, *Biochim. Biophys. Acta 942*, 215−219.
41. Sachs, G., and Munson, K. (1991) Mammalian phosphorylating ion-motive ATPases, *Curr. Opin. Cell Biol. 3*, 685−694.
42. Sweadner, K. J., and Donnet, C. (2001) Structural similarities of Na,K-ATPase and SERCA, the Ca^{2+}-ATPase of the sarcoplasmic reticulum, *Biochem. J. 356*, 685−704.
43. Vagin, O., Turdikulova, S., and Sachs, G. (2004) The H,K-ATPase β subunit as a model to study the role of N-glycosylation in membrane trafficking and apical sorting, *J. Biol. Chem. 279*, 39026−39034.
44. Vagin, O., Denevich, S., and Sachs, G. (2003) Plasma membrane delivery of the gastric H,K-ATPase: The role of β-subunit glycosylation, *Am. J. Physiol. 285*, C968−C976.
45. Abe, K., Kaya, S., Hayashi, Y., Imagawa, T., Kikumoto, M., Oiwa, K., Katoh, T., Yazawa, M., and Taniguchi, K. (2003) Correlation between the activities and the oligomeric forms of pig gastric H/K-ATPase, *Biochemistry 42*, 15132−15138.
46. Munson, K., Vagin, O., Sachs, G., and Karlish, S. (2003) Molecular modeling of SCH28080 binding to the gastric H,K-ATPase and MgATP interactions with SERCA- and Na,K-ATPases, *Ann. N.Y. Acad. Sci. 986*, 106−110.
47. Ganjeizadeh, M., Zolotarjova, N., Huang, W. H., and Askari, A. (1995) Interactions of phosphorylation and dimerizing domains of the α-subunits of Na^+/K^+-ATPase, *J. Biol. Chem. 270*, 15707−15710.
48. Mendlein, J., and Sachs, G. (1989) The substitution of calcium for magnesium in H^+,K^+-ATPase catalytic cycle. Evidence for two actions of divalent cations, *J. Biol. Chem. 264*, 18512−18519.
49. Mendlein, J., Ditmars, M. L., and Sachs, G. (1990) Calcium binding to the H^+,K^+-ATPase. Evidence for a divalent cation site that is occupied during the catalytic cycle, *J. Biol. Chem. 265*, 15590−15598.
50. Yokoyama, T., Kaya, S., Abe, K., Taniguchi, K., Katoh, T., Yazawa, M., Hayashi, Y., and Mardh, S. (1999) Acid-labile ATP and/or ADP/P_i binding to the tetraprotomeric form of Na/K-ATPase accompanying catalytic phosphorylation-dephosphorylation cycle, *J. Biol. Chem. 274*, 31792−31796.
51. Peluffo, R. D., Garrahan, P. J., and Rega, A. F. (1992) Low affinity superphosphorylation of the Na,K-ATPase by ATP, *J. Biol. Chem. 267*, 6596−6601.
52. Martin, D. W., Marecek, J., Scarlata, S., and Sachs, J. R. (2000) $\alpha\beta$ protomers of Na^+,K^+-ATPase from microsomes of duck salt gland are mostly monomeric: Formation of higher oligomers does not modify molecular activity, *Proc. Natl. Acad. Sci. U.S.A. 97*, 3195−3200.
53. Hopkins, B. E., Wagner, H., Jr., and Smith, T. W. (1976) Sodium- and potassium-activated adenosine triphosphatase of the nasal salt gland of the duck (*Anas platyrhynchos*). Purification, characterization, and NH_2-terminal amino acid sequence of the phosphorylating polypeptide, *J. Biol. Chem. 251*, 4365−4371.
54. Martin, D. W., and Sachs, J. R. (1999) Preparation of Na^+,K^+-ATPase with near maximal specific activity and phosphorylation capacity: Evidence that the reaction mechanism involves all of the sites, *Biochemistry 38*, 7485−7497.
55. Yamazaki, A., Kaya, S., Tsuda, T., Araki, Y., Hayashi, Y., and Taniguchi, K. (1994) An extra phosphorylation of Na^+,K^+-ATPase by paranitrophenyl phosphate (pNPP): Evidence for the oligomeric nature of the enzyme, *J. Biochem. 116*, 1360−1369.
56. Liu, G., Xie, Z., Modyanov, N. N., and Askari, A. (1996) Restoration of phosphorylation capacity to the dormant half of the alpha-subunits of Na^+,K^+-ATPase, *FEBS Lett. 390*, 323−326.
57. Ferreira, S. T., and Verjovski-Almeida, S. (1988) Stoichiometry and mapping of the nucleotide sites in sarcoplasmic reticulum ATPase with the use of UTP, *J. Biol. Chem. 263*, 9973−9980.
58. Froehlich, J. P., and Taylor, E. W. (1976) Transient state kinetic effects of calcium ion on sarcoplasmic reticulum adenosine triphosphatase, *J. Biol. Chem. 251*, 2307−2315.
59. Lorentzon, P., Sachs, G., and Wallmark, B. (1988) Inhibitory effects of cations on the gastric H^+,K^+-ATPase. A potential-sensitive step in the K^+ limb of the pump cycle, *J. Biol. Chem. 263*, 10705−10710.
60. Eguchi, H., Kaya, S., and Taniguchi, K. (1993) Phosphorylation of half and all sites in H^+,K^+-ATPase results in opposite changes in tryptophan fluorescence, *Biochem. Biophys. Res. Commun. 196*, 294−300.
61. Sarau, H. M., Foley, J., Moonsammy, G., and Wiebelhaus, V. D. (1975) Metabolism of dog gastric mucosa. Nucleotide levels in parietal cells, *J. Biol. Chem. 250*, 8321−8329.
62. Vagin, O., Denevich, S., Munson, K., and Sachs, G. (2002) SCH28080, a K^+-competitive inhibitor of the gastric H,K-ATPase, binds near the M5−6 luminal loop, preventing K^+ access to the ion binding domain, *Biochemistry 41*, 12755−12762.
63. Fukushima, Y., and Nakao, M. (1980) Changes in affinity of Na^+- and K^+-transport ATPase for divalent cations during its reaction sequence, *J. Biol. Chem. 255*, 7813−7819.
64. Fukushima, Y., and Post, R. L. (1978) Binding of divalent cation to phosphoenzyme of sodium- and potassium-transport adenosine triphosphatase, *J. Biol. Chem. 253*, 6853−6862.
65. Shin, J. M., and Sachs, G. (2004) Differences in binding properties of two proton pump inhibitors on the gastric H^+,K^+-ATPase in vivo, *Biochem. Pharmacol. 68*, 2117−2127.
66. Shin, J. M., Cho, Y. M., and Sachs, G. (2004) Chemistry of covalent inhibition of the gastric (H^+,K^+)-ATPase by proton pump inhibitors, *J. Am. Chem. Soc. 126*, 7800−7811.

BI051342Q